AD-A177 296

DTIC SELECTED MAR 0 2 1987 D

1a. REPORT SECURITY CLASSIFICATION Unclassified		1b. RESTRICTIVE MARKINGS
2a. SECURITY CLASSIFICATION AUTHORITY		3. DISTRIBUTION/AVAILABILITY OF REPORT
2b. DECLASSIFICATION/DOWNGRADING SCHEDULE		Approved for public release; distribution unlimited
4. PERFORMING ORGANIZATION REPORT NUMBER(S)		5. MONITORING ORGANIZATION REPORT NUMBER(S) AFOSR-TR- 87-0278
6a. NAME OF PERFORMING ORGANIZATION University of Southern Californ Center for Laser Studies	6b. OFFICE SYMBOL (If applicable)	7a. NAME OF MONITORING ORGANIZATION AFOSR
6c. ADDRESS (City, State and ZIP Code) University Park Los Angeles, CA 90089-1147		7b. ADDRESS (City, State and ZIP Code) SAme as 8c.
8a. NAME OF FUNDING/SPONSORING ORGANIZATION AFOSR/NP	8b. OFFICE SYMBOL (If applicable) NP	9. PROCUREMENT INSTRUMENT IDENTIFICATION NUMBER AFOSR - 84 - 0378

8c. ADDRESS (City, State and ZIP Code) Bolling 410 Bolling AFB DC 20332-6448	10. SOURCE OF FUNDING NOS.			
	PROGRAM ELEMENT NO. 61102F	PROJECT NO. 2301	TASK NO. A1	WORK UNIT NO.

11. TITLE (Include Security Classification)
New Efficient Optically Pumped Solid State Lasers

12. PERSONAL AUTHOR(S)
Michael Bass / Milton Birnbaum

13a. TYPE OF REPORT annual	13b. TIME COVERED FROM 8/15/85 TO 8/14/86	14. DATE OF REPORT (Yr., Mo., Day) 12/10/86	15. PAGE COUNT 59 + ?

16. SUPPLEMENTARY NOTATION

17. COSATI CODES			18. SUBJECT TERMS (Continue on reverse if necessary and identify by block number)
FIELD	GROUP	SUB. GR.	Flourescence, Multichannel, Analyze

19. ABSTRACT (Continue on reverse if necessary and identify by block number)

Several new results were achieved and reported in journals and scientific conferences (see IV to VI) Of particular note was the demonstration of efficient laser operation of high dopan density Er:YAG at 2.94 μm. This laser has valuable medical and other applications.
Our work on radiation trapping in solids, while yielding interesting and useful spectroscopic results has thus far not fulfilled its earlier promise of potential utility in improving the efficiency of optically pumped solid state lasers (see VI). A paper detailing additional results of ruby fluorescence in the presence of strong R-line trapping is in preparation.
A number of new studies were begun which have already yielded fruitful results. This is our work on the diode pumping of solid state lasers (refer to V and VI). This field promises to be of considerable importance in the development of compact and efficient solid state lasers. The Optical Multichannel Analyzer has been completed and is now operational. It is expected t play an important role in our current investigations involving Er and Ho doped crystal lasers Work has begun on research of the high dopant density Ho:YAG laser. This work complements and

20. DISTRIBUTION/AVAILABILITY OF ABSTRACT UNCLASSIFIED/UNLIMITED ☒ SAME AS RPT. ☒ DTIC USERS ☐	21. ABSTRACT SECURITY CLASSIFICATION UNCLASSIFIED
22a. NAME OF RESPONSIBLE INDIVIDUAL Michael Bass	22b. TELEPHONE NUMBER (Include Area Code) (202) 767-4906	22c. OFFICE SYMBOL NP

DD FORM 1473, 83 APR   EDITION OF 1 JAN 73 IS OBSOLETE.

→ Keywords: Flourescence Multichannel Analyzers European Holmium Yag Lasers.

DTIC FILE COPY

(CONTINUED)

19. extends the Er:YAG laser research.
During the current contract year (August '86 to August '87) we plan to pursue the
Er:YAG and the Ho:YAG laser research and to continue work on diode pumped solid
state lasers.

New, Efficient Optically Pumped Solid State Lasers

Michael Bass, P.I.
University of Southern California (USC)

Milton Birnbaum, P.I.
The Aerospace Corporation
(now at USC)

Contract No. AFOSR-84-0378
for the year
August 15, 1985 - August 14, 1986

Submitted to

A. F. O. S. R.
Bolling A. F. B.
Washington, D. C.

Atten: Dr. H. Schlossberg

Table of Contents

Accesion For		
NTIS CRA&I	✓	
DTIC TAB	☐	
Unannounced	☐	
Justification		
By		
Dist Ibution /		
Availability Codes		
Dist	Avail and / or Special	
A-1		

DTIC
COPY
INSPECTED
6

I. SUMMARY

Several new results were achieved and reported in journals and scientific conferences (see IV to VI). Of particular note was the demonstration of efficient laser operation of high dopant density Er:YAG at 2.94 μm. This laser has valuable medical and other applications.

Our work on radiation trapping in solids, while yielding interesting and useful spectroscopic results has thus far not fulfilled its earlier promise of potential utility in improving the efficiency of optically pumped solid state lasers (see VI). A paper detailing additional results of ruby fluorescence in the presence of strong R-line trapping is in preparation.

A number of new studies were begun which have already yielded fruitful results. This is our work on the tunable Ti:sapphire laser (refer to V and VI). In addition, we have begun work on the diode pumping of solid state lasers (refer to V and VI). This field promises to be of considerable importance in the development of compact and efficient solid state lasers.

The Optical Multichannel Analyzer has been completed and is now operational. It is expected to play an important role in our current investigations involving Er and Ho doped crystal lasers. Work has begun on research of the high dopant density Ho:YAG laser. This work complements and extends the Er:YAG laser research.

During the current contract year (August '86 to August '87) we plan to pursue the Er:YAG and the Ho:YAG laser research and to continue work on diode pumped solid state lasers.

1

II. INTRODUCTION

In this annual report, Sections III.1 to III.4 describe progress in research activities which have not yet been incorporated into formal papers or presentations. Research projects which have been completed and reported since the inception of this program in August '84 are listed in Sections IV and V. Full reprints are included in Section VI.

III.1   Development of the Optical Multichannel Analyzer

At the time of the annual report last year, there were still com-
munication problems between the PDP 11/73 computer system and the Quantex
video processor. This prevented the data in the Quantex video processor.
This prevented the data in the Quantex from being transferred to the computer
memory. This communication problem turned out to be due to a relatively minor
protocol difference between the PDP 11/73 and the computer which was used in
the system developed by Aerospace. Although the fix to the problem was
straightforward once identified, the search for the problem was time-
consuming, even with the help of the equipment manufacturers involved. This
problem was corrected, and communication between the Quantex and the computer
was established.

The Quantex can now be accessed by the computer, both to set the parame-
ters for image acquisition and to return the digitized video image for addi-
tional processing by the computer. One of the features which exists in the
software allows the user to subtract a background signal from another video
image. In this manner very weak signals from the camera can still be used,
since the background noise levels can be subtracted out of the total signal to
extract a small signal. A single video frame received from the television
camera is represented as a 512 by 512 array of picture elements, or pixels. A
horizontal line across the face of the camera tube consists of a linear array
of 512 elements. The spectrometer is set up so that the spectral lines pro-
duced are vertical with respect to the camera tube. When this alignment is
done carefully, if pixel #387 on a horizontal line near the top of the image
corresponds to the peak of an emission line, then pixel #387 on a line near

3

the bottom of the screen will also correspond to the same peak. This has been done with the instrument. This allows a number of horizontal lines to be averaged to further improve the S/N ratio. This line averaging software now exists on the computer and does yield an improved S/N ratio.

Graphics have been added to the software which allow the user to view any given horizontal or vertical line scan as a graph of amplitude vs. line position. This graph can be displayed for a single line or for the average of many lines. More than one graph can be displayed on the same set of coordinate axes for ease in comparing data. The portion of the data which is displayed is also controlled by the operator. A section of the horizontal scan can be viewed if the entire line is not required. The amplitude scale can also be chosen by the user. With this window feature, some of the details of the data can be expanded for greater clarity.

Through the use of spectral calibration lines such as those provided by a mercury vapor light source or laser lines from ion lasers, the OMA assembly can be calibrated. This allows a given pixel position to be assigned a particular wavelength value. With two or more calibration lines in the field of view of the camera and a knowledge of the dispersion of the grating, the entire image field can be calibrated for wavelength. The graphics now allow a wavelength scale in nanometers to be displayed on the horizontal axis. A scale which reads in cm^{-1} will be added to the software package for convenience.

It was discovered that the scaling of the data is very sensitive to the alignment of the camera and the spectrometer. For this reason it will not be

4

possible to simply use the counter provided on the monochromator to dete :ine the scale for the data. If the camera were to shift between runs, there would be an offset in the wavelength scale. This means that the calibration of the device will have to be checked before each data run is made. It does not seem likely at this time that it will be possible to automate calibration.

The OMA assembly seen in Figure 1 consists of the PbS camera, the monochromator, and a mounting fixture to hold these two components in a fixed position with respect to one another. As has already been discussed, this is not a perfectly rigid mount, and some play does exist, necessitating frequent calibration checks. The mounting fixture allows for roll adjustment to ensure that the spectral lines are aligned with the camera vertical. The pitch and yaw adjustments permit top-to-bottom and right-to-left focusing corrections, respectively. The camera sits on a tilt table constructed to permit x, y, and z translation as well as two of the angular adjustments. The z-axis translation is by means of a translation stage which interfaces to the camera body. This permits delicate and precise focusing of the spectrum produced by the monochromator.

The camera is being used without any lenses, and the spectrum is imaged directly onto the surface of the camera tube. This provides for a stronger signal, as none of the light will be lost by intermediate optics. This is particularly important in the region near 2 μ, where some of the signal would be absorbed by the glass in the lens. One problem which exists with the system in its present form is that the field of view of the monochromator in the focal plane (the monochromator is being used without an exit slit, effectively making it a spectrometer) is smaller than the field of view of the

5

camera. This results in a shadow region at both edges of the video image, as these portions of the camera tube are not being used. The camera tube is underfilled in the horizontal dimension, but no clear solution to this problem exists at this time.

The monochromator which is in use is a 1/4-meter monochromator manufactured by Jarrell-Ash. The grating which is used for the studies of the ~ 1.5 μ fluorescence of the Er:YAG has 300 lines/mm and is blazed for 2 μ. There are plans to adapt the camera and its tilt table for use with a 1/2-meter instrument to obtain higher resolution. These plans will proceed in the next few months. The computer is also interfaced with an HP 7475A six-pen plotter. This plotter produces hardcopy graphs of the data which has been acquired and processed by the system. A plot of a portion of the emission spectrum of Er:YAG near 1.5 μ is shown in Figure 2. This spectrum was taken in a spectral region which is n ot accessible by the silicon detectors which such commercial devices use and demonstrates the unique capability of this device over a commercial OMA device. This system is now in use to study the visible and near IR emission spectra of Er:YAG and Ho:YAG laser materials.
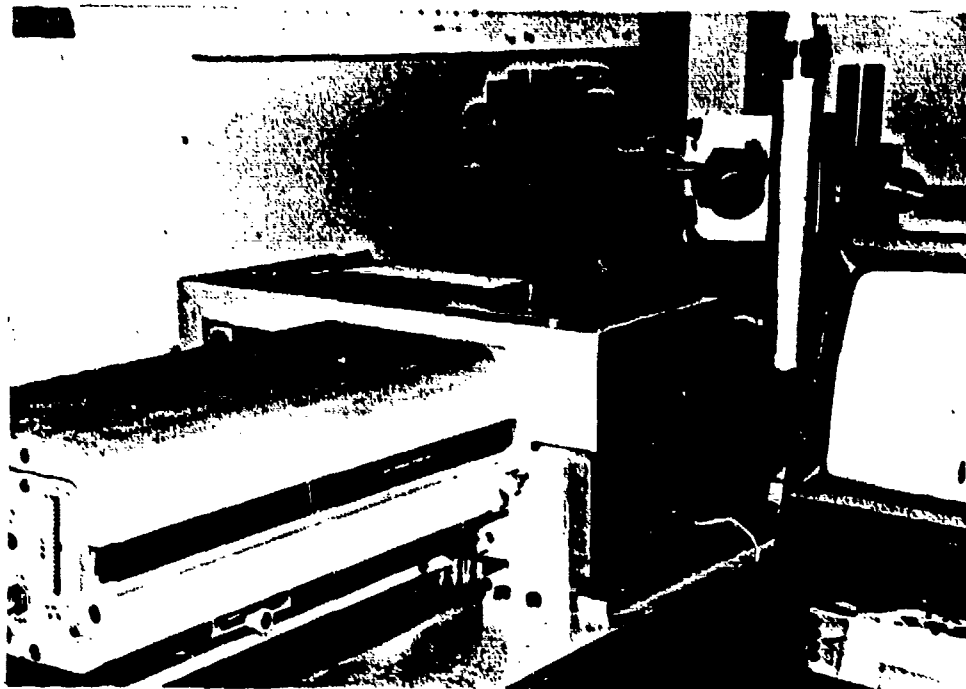
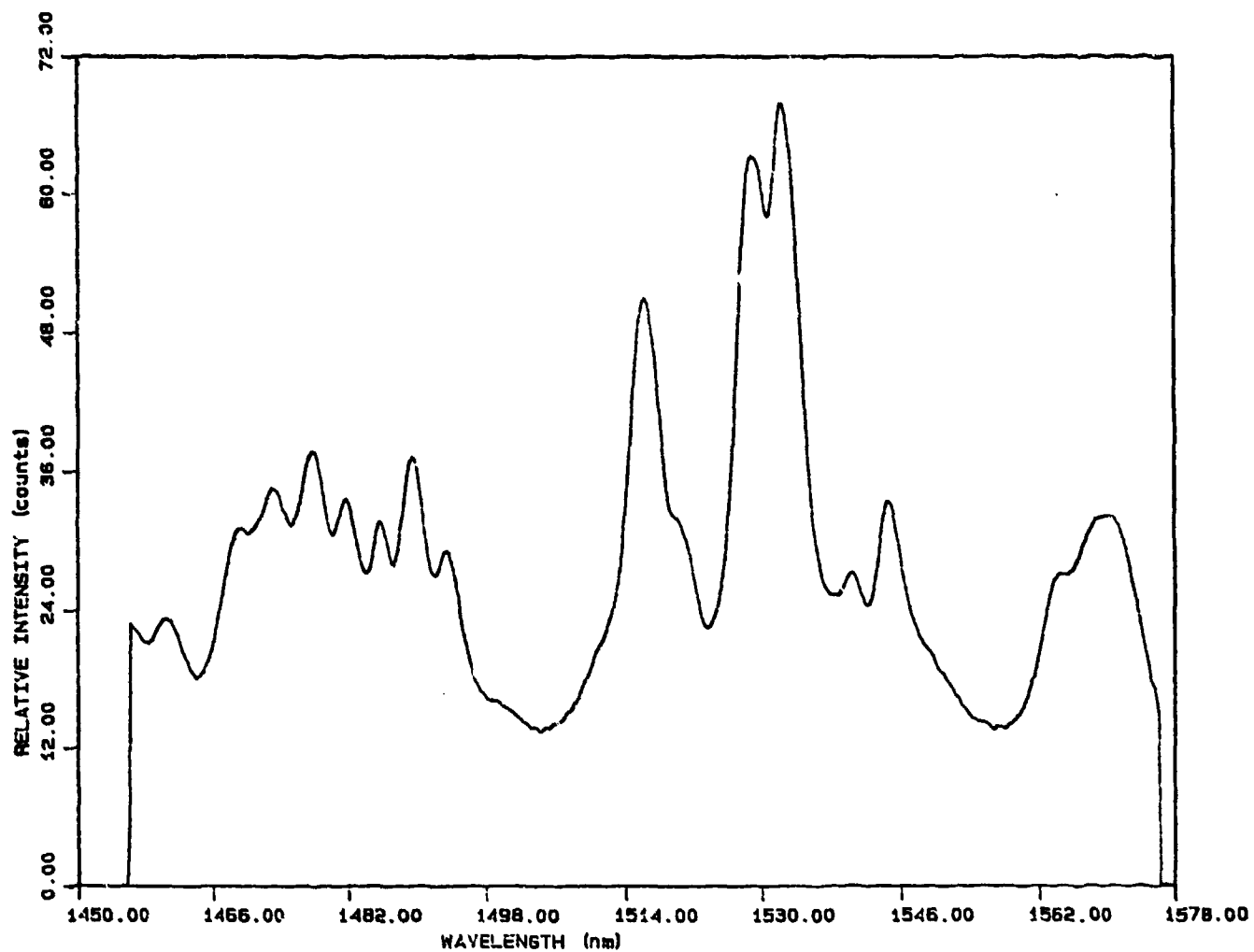Figure 1. Two views of the Optical Multichannel Analyzer

Figure 2.   Emission Spectrum of 50% Er:YAG Near 1.5μ

III.2   Ho:YAG Laser

While the work on the high-concentration Er:YAG continued during the past year, the prospects for another three micron lasers were investigated. Holmium-doped YAG has been shown to lase near 3 μ at room temperature. This transition occurs between the $^5I_6$ and $^5I_7$ levels in holmium. This transition is self-terminated because the lower laser level has a longer lifetime than the upper laser level. This results in a laser which can only be operated in a pulsed mode, and which has a reduced efficiency since the lower level does not empty out quickly.

Several schemes are being considered in order to achieve more effici-nt operation of a holmium-doped YAG crystal on this 3 μ transition. Better use of the pump light can be accomplished either by doping the crystal more heavily with the activator ion, or by using other ions as sensitizers. These sensitizers subsequently transfer their energy to the active ion. A second approach is to reduce the lifetime of the lower laser level. This can result from concentration quenching of the level in question, or from the addition of other ionic species to the crystal.

An extensive study of the literature has revealed some past work in this area, and has suggested several possible research areas. Soviet researchers have synthesized Ho:YAG crystals with holmium concentrations up to 100% (holmium aluminum garnet). These studies show that the upper laser lifetime remains virtually unchanged throughout this entire range, while the $^5I_7$ lifetime decreases from about 8 to 0.3 msec in the pure holmium garnet. This would suggest that the pure garnet might be a more efficient laser material than crystals with low holmium concentrations.

9

Very limited data is available on the lasing properties of any of these crystals. The lasing wavelengths of YAG crystals with holmium concentrations of up to 15 at .% are given, but there is no information on the output energies or efficiencies of these lasers. One Soviet paper[2] reports that lasing could not be obtained from crystals with > 20% holmium, but studies were not done which could determine the reason for this behavior. No spectroscopic studies of these crystals exist in the literature, so studies of holmium-doped YAG will be conducted at several activator concentrations. Spectroscopy will be used to study the properties of the 3 μ transition as a function of activator concentration. The lasing properties of those crystals which can be made to lase will be studied. Crystals doped with ~ 15% holmium have been ordered from Union Carbide, and are expected shortly.

In addition to the reduction in the $^5I_7$ lifetime due to concentration quenching, it may be possible to unblock this level through the use of a deactivator ion. Studies done in BaY_2F_8 have shown that the lower state lifetime of the 3 μ holmium transition could be reduced by more than an order of magnitude with the addition of ~ 1% of either europium or praseodymium to the crystal.[3] This reduction was accomplished with little effect on the upper level lifetime at this doping level.

To our knowledge no similar studies have ever been undertaken in a garnet. It has not been demonstrated whether such a deactivating scheme can improve the efficiency or permit cw operation of holmium lasers at 3 μ. This is an area which should be explored. Soviet researchers have also suggested that neodymium could be used to reduce the lifetime of the lower laser level, but experimental results have not been published. The specific deactivator

which will be used has not been decided on, but an attempt at such a scheme is being considered.

III.3   Er:YAG Laser

Analysis of the results reported (see VI, reprint 2) has yielded significant new insights into the operation of the high dropout density (50%) Er:YAG laser. By solving the rate equations for this laser, good agreement was obtained between the predicted and observed performance (see reprint 20. This satisfactory agreement was obtained by assuming a cross-relaxation rate a factor of ten less than that given in Ref. 1 (end of III.3).

This is an example of a self-pumping process which occurs in Er:YAG because of the near energy coincidence of the transitions 9/2 to 13/2 and 13/2 to 15/2. This is denoted by W3 on Fig. III.3-1. In this process, two Er^{3+} vacate the 13/2 level at the practically the same instant - one drops down to the 15/2 level and the other goes up to the 11/2 level. It is clear that both a high concentration of Er^{3+} and near coincidence in energy of the two transitions favor this process. This action is very favorable for improving the efficiency of the Er:YAG laser since each W3 event (Fig. III.3-1) reduces the population of the 13/2 by 2 while increasing the upper laser level population by 1.

For a given host crystal and concentration of Er^{3+}, the rate of the W3 process is fixed (assuming a particular temperature). However, by analysis we can examine the value of this parameter which leads to long pulse operation and perhaps even CW operation. Alternatively, the value of the parameter W3 which results in agreement with the experimental results suggests that our experiments provide a new method for estimating this parameter. Additional experiments with other concentrations of Er^{3+} in Er:YAG and further analysis are in order to clarify our model for the 2-9 μm er:YAG laser.
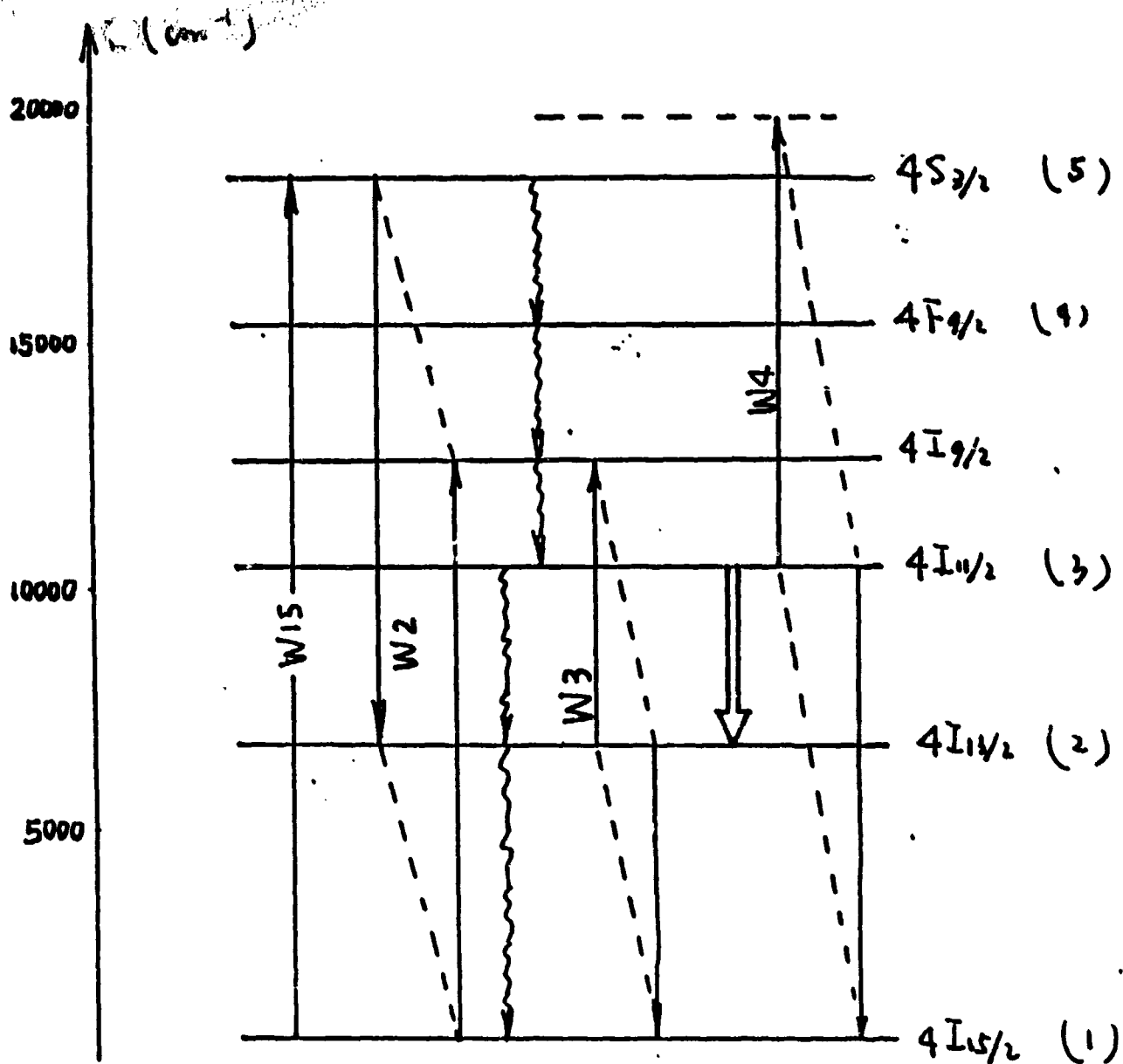
12

Fig.3. Energy level diagram of Er:YAG and various transitons

III.4   Radiation Trapping in Ruby

A report is in preparation which describes our observations of the fluorescence of ruby under strong trapping of the 0-phonon lines over the temperature range of 77 to 300 K. A major conclusion is that the lifetime of the vibronic transitions follows a dependence similar to that of the 0-phonon lines or R-lines. Apart from the preparation of this paper, further work along these lines during this contract year is not anticipated.

References

1. The Aerospace Corporation, P. O. Box 92957, El Segundo, California, 90009.

2. V. I. Zhekov, V. A. Lobachev, T. M. Murina, and A. M. Prokhorov, Sov. J. Quantum Electronics, Vol. 11, No. 2, pp. 279-281.

3. L. F. Johnson and H. J. Guggenheim, IEEE J. Quantum Electronics, Vol. QE-10, No. 4, pp. 442-449, April 1974.

4. A. A. Kaminskii, T. I. Butaeva, A. O. Ivanov, I. V. Mochalov, A. G. Petrosyan, G. I. Rogov, and V. A. Fedorov, Soviet Technical Phys. Lett., Vol. 2, No. 9, pp. 308-310, September 1976.

IV. Publications and Papers

1. Alexander, J. Portica, "CW Operation of the Ti:Sapphire Laser," M.S. Thesis, Physics, August 1986.

2. Milton Birnbaum, Curtis L. Fincher, Jason Machan and Michael Bass, Radiative Trapping Effects in Ruby: 77K to 300K, to be published in JOSA B, December 1986.

3. M. Bass, W. Q. Shi, R. Kurtz, Center for Laser Studies, University of Southern California, Los Angeles, CA 90089-1112, M. Kokta, Union Carbide Corporation, Washougal, WA, and H. Diegl, Allied Corporation, Westlake Village, CA, "Operation of the High Dopant Density Er:YAG at 2.94 μm" to be published in Proceedings of the Tunable Solid State Laser Conference, Zig-Zag, Oregon, May 1986.

4. R. A. Fields, M. Birnbaum, and C. L. Fincher, Electronics Research Laboratory, The Aerospace Corporation, P. O. Box 92957, Los Angeles, CA 90009, "Highly Efficient Diode Pumped Nd:Crystal Lasers."

5. Milton Birnbaum, Center for Laser Studies, University of Southern California, Los Angeles, CA 90089, and Alexander J. Pertica, now at Lawrence Livermore National Lab., University of California, Livermore, CA 94550, "Laser Material Characteristics of Ti:Al$_2$O$_3$."

6. Milton Birnbaum, Curtis L. Fincher, Jason Machon and M. Bass, "Ruby Fluorescence with Radiative Trapping," in preparation.

V. Meetings and Talks

OSA, Seattle, WA, October, 1986 (IV-2).

Tunable Laser Conference, May 1986, Zig-Zag, OR (IV-3).

CLEO/IQEC '86, May 1986, San Francisco, CA (IV-3).

Submitted for presentation: CLEO '87, Baltimore, MD, May '87 (IV-4).

Submitted for presentation: CLEO '87, Baltimore, MD, May '87 (IV-5).

VI. Reprints of Publications

IV-2.

IV-3.

IV-4.

IV-5.

Radiative Trapping Effects in Ruby: 77K to 300K

Milton Birnbaum and Curtis L. Fincher

The Aerospace Corporation

P. O. Box 92957

Los Angeles, CA 90009

and

Jason Machan and Michael Bass

Center for Laser Studies

Los Angeles, CA 90007

ABSTRACT

The fluorescent decay of the 2_E level of the Cr^{3+} over the range of 77°K to 300°K has been studied in experimental arrangements providing strong trapping of the O-phonon lines. At 300°K, rubies as large as 2.5 cm diameter by 28 cm length were used and were packed in highly reflective $BaSO_4$ powder to provide adequate trapping of the O-phonon fluorescence. The measurements resulted in the determination explicitly of the lifetime vibronic transitions and the O-phonon decay rate. These studies of lifetime enhancement have potential application in the design of efficient solid-state lasers.

Introduction

Radiative trapping effects are important in the operation of lasers. A well known example is the Cu vapor laser[1] where radiative trapping of the pump radiation is utilized to increase the lifetime of the pumped level and thereby alleviate the stringent requirements on the rise time and duration of the pump pulse. In general, radiative trapping effects in solids are less pronounced than in gases because of the difficulty of meeting the requirement that the emitted fluorescence be resonantly reabsorbed. In ruby, Nelson and Sturge[2] showed that self-absorption of the fluorescence (radiative trapping) could be used to obtain the lifetime of the vibronic transitions for the ^2E upper level. We have extended their results and have obtained the lifetime associated with the vibronic transitions at 77K and 300K and explicitly the lifetimes of the O-phonon transitions.

Theoretical Considerations

The spectroscopy of the R-line fluorescence in ruby has been extensively studied,[2] stimulated by the utility of ruby as a laser material (in fact, the first laser). The relevant aspects of the energy level diagram and the fluorescence emissions are shown, respectively, in Figs. 1 and 2. The R_1 and R_2 line emissions are O-phonon lines[2] and strong reabsorption (trapping) can be readily obtained.

An estimate of the magnitude of the radiative trapping effect was obtained from the analysis of Holstein.[3] For a Gaussian line with a peak absorption coefficient of α_m, Holstein finds that in a long cylinder of radius R the lifetime is lengthened by the factor

$$\tau_{tr}/\tau_{utr} = 0.63\alpha_m R \, [\ln(\pi\alpha_m R/2]^{1/2} \qquad (1)$$

where τ_{tr} = the trapped or lengthened lifetime and τ_{utr} = the untrapped life-time. In a ruby crystal of practical dimensions (5/8" diameter by 7.5" length) Eq. (1) predicts that an opaquely silvered rod will show a large lifetime lengthening factor (practically complete trapping of the O-phonon lines of ruby at 77K).

The observed lifetime, τ_{obs} of the red-line fluorescence is given by

$$1/\tau_{obs} = 1/\tau_1 + 1/\tau_2 + 1/\tau_3 \qquad (2)$$

where τ_1 is the lifetime of O-phonon lines, τ_2 the lifetime of the vibronic lines and τ_3 the non-radiative lifetime of the fluorescing levels. For the case of strong trapping, $\tau_1 \gg \tau_3$, τ_2 and $1/\tau_{obs} = 1/\tau_2 + 1/\tau_3$. From spectro-scopic studies, τ_3 can be estimated, thereby leading to a determination of the lifetimes of the vibronic lines, τ_2. At 77K, the lifetime τ_2 of the vibronic lines is much shorter than that of the non-radiative lifetime τ_3 leading to the expression $1/\tau_{obs} = 1/\tau_2$ and a direct measurement of τ_2.

Experimental Method

A block diagram of the experimental arrangement is shown in Fig. 3. A cold finger arrangement was utilized for measurements of the smaller rubies (see Table 1) over the temperature range of 77-300K. The larger rubies (Table 1) were studied at 300K only.[†] All samples in this work had Cr^{3+} concentra-tions of ~0.05%. At 77K, data was obtained with bare ruby rods and opaquely silvered ruby rods with small apertures to introduce the pumping radiation and

to allow exit of the fluorescence. The fluorescence was excited by chopping the output of a Spectra-Physics CW argon ion laser operating at 514.5 nm. The exciting pulse duration was short in comparison to the fluorescent lifetimes. The ruby rods (3/4" x 10" and 1 x 13"), were measured at room temperature only. The were packed tightly in a $BaSO_4$ powder which provided a diffuse reflectivity greater than 99.5%.[††] For the 10" ruby rod (and similarly the 13" ruby rod) the excitation light input port as well as the observation ports were thin optical fibers attached with an optical cement (Fig. 4).

The experimental arrangement for the large rods is shown in Fig. 4 and is similar to that of Fig. 3. The additional feature of Fig. 4 was the utilization of a computerized data acquisition system whose major components consisted of a Tektronix Digital Processing Oscilloscope (DPO), a Hewlett-Packard 9825A computer and a Hewlett-Packard 9872 X-Y plotter. A typical example of the data obtained is shown in Fig. 5 in which the fluorescence data of 100 pulsed excitations were averaged. In general, the precision of a lifetime measurement was about 4%. The fluorescence lifetime measurements of rods 5 and 6 were taken at exit ports near the excitation port and the most distant ports. The observed lifetimes were maximum towards the far end of the rod and exhibited saturation, namely, the lifetime observed at the three most distant ports were nearly identical. This was observed for rods 5 and 6. The lifetimes listed in Table 1, column 4 in rods 5 and 6 refer to the saturated value.

A less precise procedure was employed for the smaller rods when using the arrangement of Fig. 3. Here the fluorescent decay was displayed on an oscilloscope and was photographed. The decay was determined by direct measurement of the photographed decay curve. The results obtained by this procedure were compared with those obtained with the computerized data acquisition system of

4

Fig. 4. For a set of measurements on different small rods, the direct oscill-ograph measurements agreed with those obtained with the computerized data acquisition system, utilizing signal averaging, to 3%. However, on the average the lifetimes were measured to a precision of about 7% when utilizing the direct measurement system of Fig. 3 based upon the repeatability of the results. Nelson and Sturge[2] found that the fluorescent decays were not strictly exponential initially, but became accurately exponential after the first 6 msec. We have corroborated these observations. The values reported here refer to this strictly exponential decay.

Experimental Results

The relevant measurements obtained and the derived lifetimes are summar-ized in Table 1. The precision of the measured values for the first four rows is approximately 7% and that of the last two rows is ~4%.

In Table 1, the values of τ_{obs} and τ_2 for rows 1 through 4 are identi-cal. The non-radiative lifetimes of the ^2E level in ruby at 77K are very long compared to τ_1 and τ_2.[2] Under conditions of strong trapping of the O-phonon lines, $\tau_1 \gg \tau_2$, τ_3; thus $\tau_{obs} = \tau_2$, as shown in Table 1. In order to verify the strong trapping assumption, ruby rods 3 and 4 were opaquely silvered. The values obtained for τ_{obs} at 77K, were in good agreement. The value of "R" to be used in Eq. (1) to estimate the lifetime lengthening factor is increased by a factor of 80 in comparison to the unsilvered ruby rod. These experiments were important in demonstrating that the trapping of the O-phonon lines in ruby was large enough to ensure that $\tau_1 \gg \tau_2$, τ_3. This condition could be achieved with rods 5 and 6 at 300K when encapsulated in the $BaSO_4$ powder and was experimentally verified by the results obtained with ruby rods 5 and 6. The fact that the same lifetimes were obtained for both rods indicated that

5

complete trapping of the O-phonon radiation had already been achieved in rod 5, the smaller of the two.

The last two rows of Table 1 at 300°K summarize our measurements on the two very large ruby rods. The values of τ_{obs} (4th column, Table 1) sum the vibronic and non-radiative contributions to the lifetime.

Table 1. Lifetimes of Fluorescent Emissions in Ruby

Ruby No.	T (K)	Dimensions (in.) diam. × length	τ_{obs} trapped (ms)	τ_1 (ms)	τ_2 (ms)
1	77	3/8 × 9/8	15.4	6.0	15.4
2	77	1/4 × 3/2	16.6	5.8	16.6
3	77	1/4 × 2	15.5	6.0	15.5
4	77	1/2 × 2	16.8	5.8	16.8
5	300	3/4 × 10	8.4	5.4	14.5
6	300	1 × 13	8.7	5.3	15.4

τ_{obs} = experimentally observed lifetime (nearly complete trapping)
τ_1 = R-line lifetime, O-phonon line (untrapped)
τ_2 = R-vibronic lines lifetime

The values of Table 1 for the spontaneous decay rates, τ_1 and τ_2, are slightly smaller at room temperature than at 77K. This result is expected since at room temperature there is a small but appreciable population in the $^2T_1$ level, ~500 cm^{-1} above the metastable ^2E level. The radiative decay of the $^2T_1$ is much faster than that of the ^2E level and this could account for the reduced lifetimes at room temperature.

The values of columns 5 and 6 of Table 1 were obtained with the aid of Eq. (3),

$$1/\tau_{utr} = 1/\tau_1 + 1/\tau_2 + 1/\tau_3 \qquad (3)$$

where τ_{utr} is the untrapped lifetime and τ_3, the lifetime of the non-radiative transitions. The values of τ_{utr} are 4.3 and 3.3 ms at 77 K and 300 K respectively.[2] At 77 K, τ_3 is much greater that τ_1 and τ_2 and can be neglected in Eq. (3), while at 300 K, $\tau_3 = 20$ ms[2]. At 77 K, $1/\tau_{obs} = 1/\tau_2$ since $\tau_1 \gg \tau_2$. Therefore $\tau_2 = \tau_{obs}$ for the first 4 rows of Table 1. To obtain τ_1, we note that $1/\tau_{utr} = 1/\tau_1 + 1/\tau_2$ or $1/\tau_1 = 1/\tau_{utr} - 1/\tau_{obs}$. The results listed in Table 1 for the large rubies at 300 K can be obtained similarly: $1/\tau_1 = 1/\tau_{utr} - 1/\tau_{obs}$ and, therefore $1/\tau_2 = 1/\tau_{obs} - 1/\tau_3$.

Conclusions

The fluorescent decay of the ^2E level of the Cr^{3+} over the range of 77K to 300K has been studied in experimental arrangements providing strong trapping of the 0-phonon lines. This has resulted in the determination explicitly of the lifetime of the vibronic transitions, τ_2, and the 0-phonon decay rate, τ_1.[†††]

References

1. L. A. Weaver, C. S. Liu, and E. W. Sucov, _IEEE J. Quantum Electron_ QE-10, 140, 1974.

2. D. F. Nelson and M. D. Sturge, "Relation Between Absorption and Emission in the Region of the R-Lines of Ruby," _Phys. Rev._ 137, No. 4A, 15 Feb. 1965, A1117-A1130.

3. T. Holstein, "Imprisonment of Resonant Radiation in Gases," _Phys. Rev._ 172, 1212 (1947).

List of Figures

Figure 1. Electronic energy levels of Cr^{3+} in Al_2O_3.
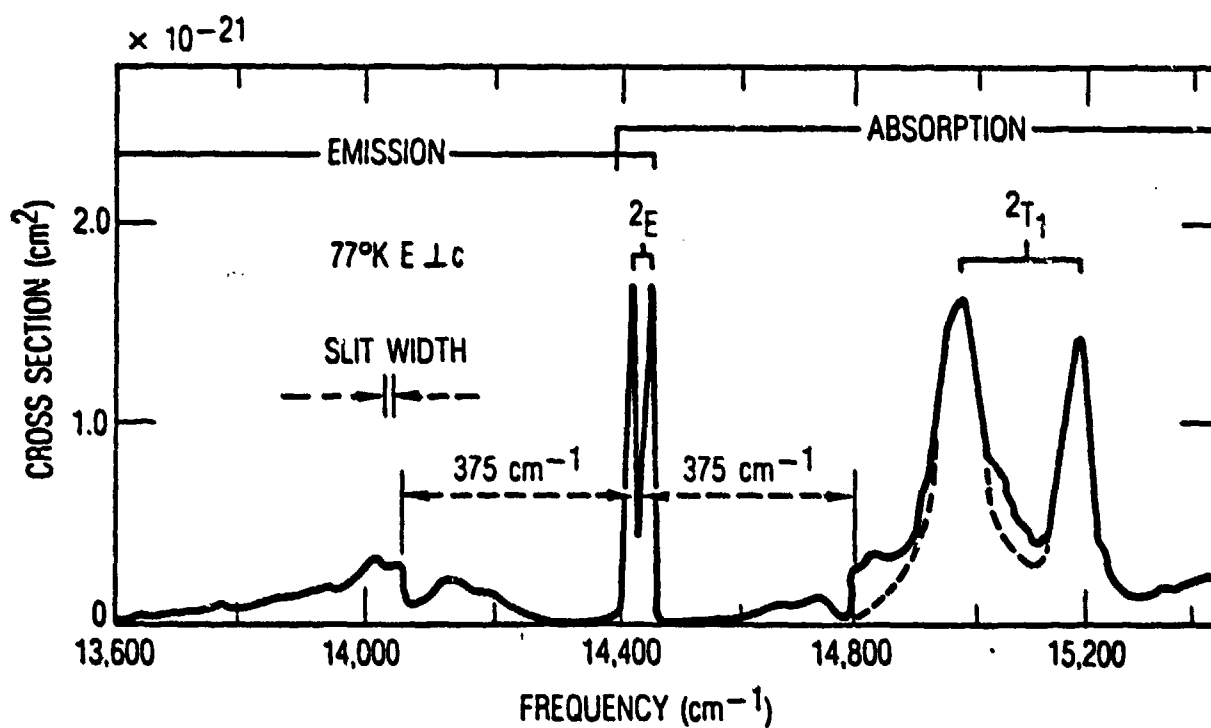
Figure 2. Emission and absorption (actually excitation) spectra of dilute ruby in the vicinity of the R lines at 77°K (E⊥C).[2]
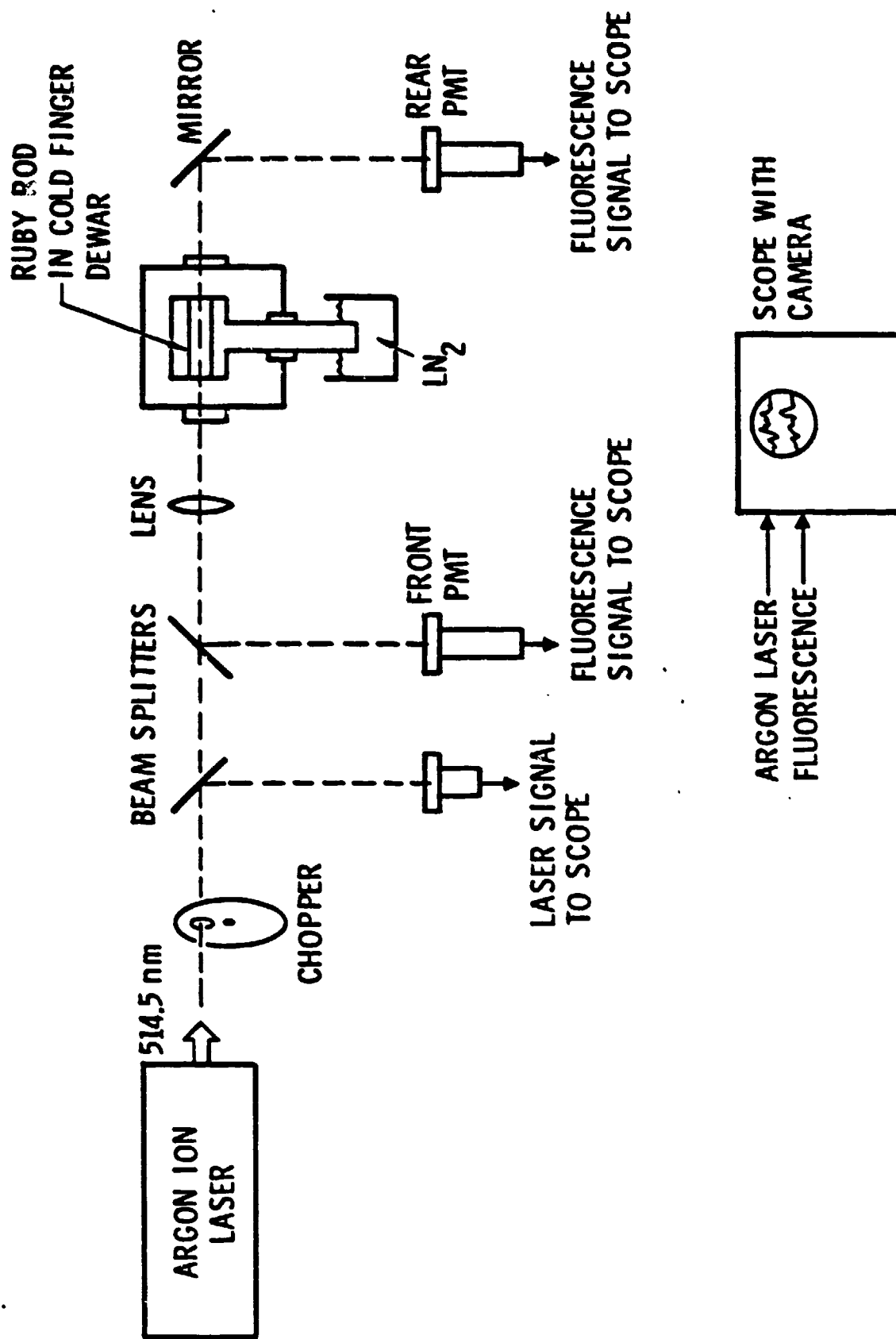
Figure 3. Experimental arrangement for fluorescence lifetime measurements, 77°K to 300°K.

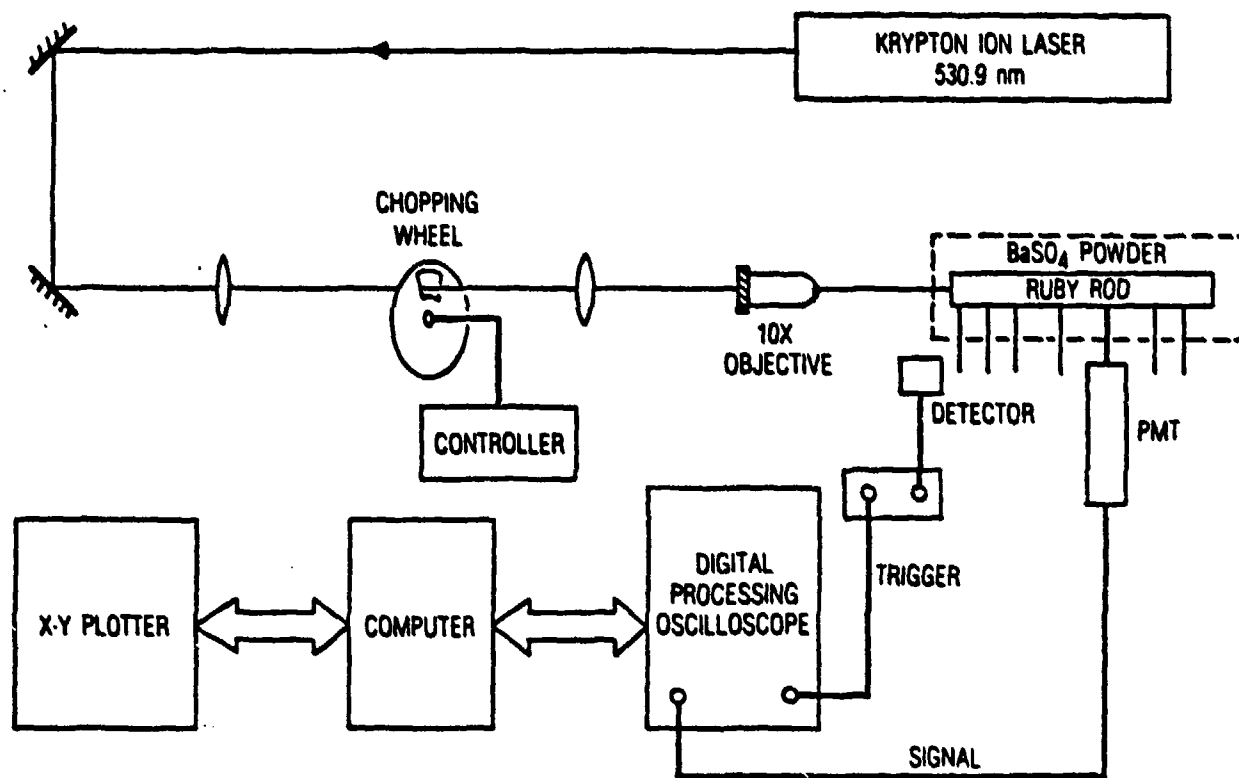Figure 4. Experimental arrangement for measurements of fluorescence
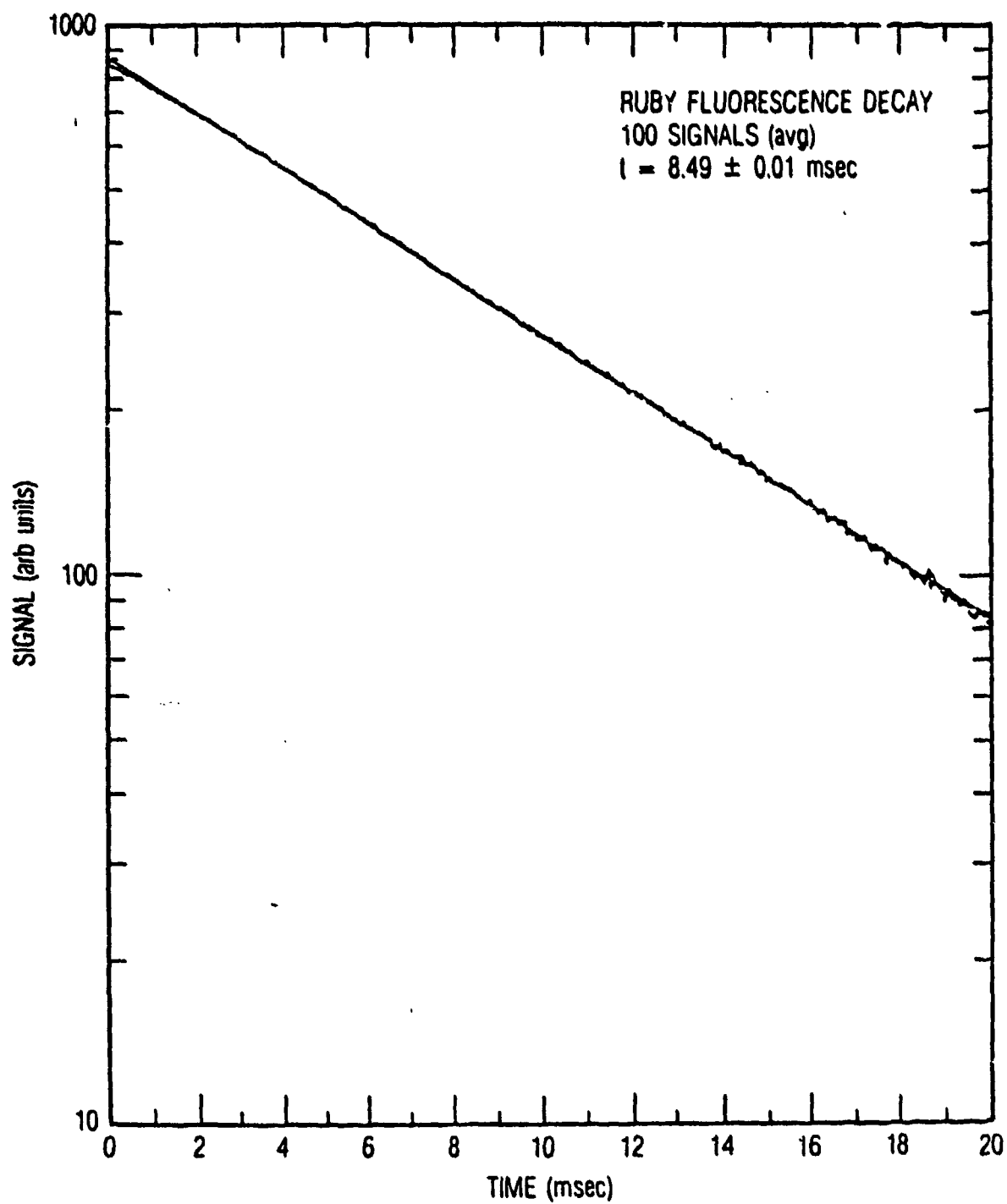lifetimes at 300°K utilizing a computerized data acquisition
system.

Figure 5. Fluorescence decay data of ruby rod, No. 5 (Table 1) at $300°K$ when the R line fluorescence is strongly trapped.

14

OPERATION OF THE HIGH DOPANT DENSITY ER:YAG AT 2.94 μm

M. Bass, W. Q. Shi, R. Kurtz
Center for Laser Studies
University of Southern California
Los Angeles, CA 90089-1112

M. Kokta
Union Carbide Corporation
Washougal, WA

H. Diegl
Allied Corporation
Westlake Village, CA

1. Introduction

Free running, pulsed, flashlamp excited operation of 50 and 33% Er doped YAG lasers is reported at 2.94 μm. This laser was described by researchers in the Soviet Union as early as 1975.[1] Since then there have been a number of further reports concerning this material all published by Soviet scientists. This paper represents, to our knowledge, the first publication outside of the Soviet Union about high dopant density Er:YAG laser operation. In addition to confirming some of the performance properties described earlier, this paper presents the unusual temporal waveforms of the Er:YAG, 2.94 μm laser. An outline is given of possible pumping and relaxation processes which may contribute to the laser's operation.

Er:YAG does not lase well at 2.94 μm when the concentration of Er is the usual 1%. However, when larger concentrations are used (generally over 15%) operation at this wavelength can be quite efficient. The relevant spectroscopic data for lasing at this wavelength are given below for 50% Er:YAG:

Upper laser level	$^4I_{11/2}$
Lower laser level	$^4I_{13/2}$
Upper level lifetime	100 μsec

Lower level lifetime	2 msec

Emission cross section	2.6×10^{-20} cm^2

Pump absorption bands

0.80 μm   ($^4I_{15/2}$ - $^4I_{9/2}$)

0.65 μm   ($^4I_{15/2}$ - $^4F_{9/2}$)

0.54 μm   ($^4I_{15/2}$ - $^4S_{3/2}$)

0.52 μm   ($^4I_{15/2}$ - $^2H_{11/2}$)

0.49 μm   ($^4I_{15/2}$ - $^4F_{7/2}$)

0.45 μm   ($^4I_{15/2}$ - $^4F_{5/2}$)

0.44 μm   ($^4I_{15/2}$ - $^4F_{3/2}$)

0.41 μm   ($^4I_{15/2}$ - $^2H_{9/2}$)

0.38 μm   ($^4I_{15/2}$ - $^4G_{11/2}$)

2. Laser Tests

The laser tests were conducted in a water cooled, double elliptical pump cavity. This cavity had been designed for pumping Alexandrite laser rods and so had the desired silver backed pyrex reflector. While the laser may work in a gold plated cavity, the many visible, blue and near uv pump bands suggest better efficiency is possible with a silver pump reflector. The rods reported in this paper were 6.25 mm in diameter and 120 mm long. They were obtained from Union Carbide Corp. and Crystal Optics Research Inc. The flashlamps were 6.5 mm bore diameter, xenon filled lamps from ILC and, in the pump cavity used, were able to pump 96.5 mm of the rod. Two different pump pulse durations were used; one, called the short pump pulse, was 120 μsec long at full width at half maximum (FWHM) and the other, called the long pump pulse, was 170 μsec FWHM. The resonators mirrors were spaced only 25 cm apart to provide a resonator that was relatively insensitive to thermal lensing in the laser rod. The 100% reflector used was an uncoated, polished copper mirror with a 5 m radius of curvature. Several flat output mirrors were tested but best performance was observed for all rods with a 75% reflector. All tests were conducted with no intracavity apertures and so represent long pulse, multimode lasing in which the whole rod aperture was filled with many oscillating modes.

The performance of the Er:YAG lasers tested is summarized in Figs. 1 and 2. Fig 1 a compares the performance of the 33% doped rod when pumped with the two different pump pulses mentioned above. The

improvement in efficiency as the pump pulse duration is increased agrees with observations reported previously[2] and suggests that the reported 3-5% efficiencies are realizable. Fig. 1b shows the relative performance of the 33 and 50% doped rods. when pumped with the long pump pulse. The difference observed may be specific to the pump pulse waveform and pump cavity used in this work. The performance differences may depend on these parameters and so this data should not be taken as a firm preference for the 33% rod over the 50% rod. More research is necessary with excitation conditions properly tailored to the rod to be used. Both rods showed excellent optical quality when observed through crossed polarizers and no significant scattering of a HeNe beam could be detected. It should be noted that the 0.63 μm HeNe beam is attenuated in Er:YAG but the orange HeNe line is transmitted and should be used.

Fig. 2 shows the average power obtained using the 33% rod and the short pump pulse. These tests were limited by power supply considerations and it is clear that much higher average powers are possible. When the long pump pulse was used the maximum power supply repetition frequency was 3 Hz. At this prf over 5 W of average power was observed. The drop off in energy per pulse indicates the onset of thermal lensing in the medium. Since no corrective measures were taken other than using a short resonator this problem can benefit from further laser engineering.

A major design consideration in developing this laser is preparing reliable, damage resistant optical coatings. The major coating consideration is that the material not contain any water when it is set down and that it not adsorb water from the atmosphere afterwards. The absorption of water at 2.94 μm is maximum and so any water in a coating causes unacceptably high losses and low damage threshold. High reflection coatings were reliably produced by coaters who had experience in making coatings for HF and DF lasers. On the other hand, only one manufacturer made reliable AR coatings for the laser rods. These coatings performed reliably at pulse energies of over 1.7 J. AR coatings supplied by another manufacturer damaged at outputs of less than 250 mJ. In fact, the data given in Figs. 1 and 2 were taken with uncoated rods to avoid the issue of coating properties.

The waveform of the laser emission of Er:YAG at 2.94 μm is somewhat like that of any conventional optically pumped solid state laser near threshold. Fig 3 shows the observed waveform at

threshold using the short pump pulse. The important point is that there are relaxation oscillation (RO) spikes and that lasing begins after the peak of the pump pulse. When this laser is pumped well above threshold with either the long or the short pump pulse the output waveform is as shown in Fig. 4. The Er:YAG laser waveforms shown in Figs. 3 and 4 were obtained with a Judson Infrared J-10 InSb detector, cooled to 77 °K, with a specified response time of 500 nsec. These waveforms were subsequently verified with a 50 nsec response time Judson Infrared Model J-12-18C-R250U InAs room temperature detector.

In the case of Fig. 4 lasing begins before the peak of the pump and ends when the pump is nearly over. In between it operates nearly continuously without RO spikes typical of optically pumped solid state lasers. This type of RO spike does not appear until the pump has fallen well below threshold. It is expected that the improved performance reported for longer pump pulses is related to this mode of lasing in which some process operates to alter and extend the population inversion.

3. Discussion

The long pulse performance of the Er:YAG laser in terms of both energy per pulse and average power has been shown to be comparable to other optically pumped solid state lasers. Higher outputs and efficiencies can be expected using longer duration pump pulses.[3]

The unusual waveforms observed at high output energies are the result of a combination of processes. These include contributions to the inversion due to:
1, the usual "four-level" pumping process involving excitation from the $^4I_{15/2}$ ground state,

2, "three level" pumping from the long-lived lower laser level, the $^4I_{13/2}$ state, and

3, cross relaxation between nearby Er^{3+} ions. The cross relaxation process is one in which an ion in the $^4I_{13/2}$ state relaxes to the $^4I_{15/2}$ state while, simultaneously, a neighboring ion in the $^4I_{13/2}$ jumps to the $^4I_{9/2}$ state.

When in the $^4I_{9/2}$ state the ion rapidly relaxes into the upper laser level. The process of cross relaxation is particularly important in high concentration material and is discussed in detail by Bagdasarov et al.[4] An analysis is in progress of the relative importance of the several processes of excitation and relaxation as they contribute to the observed quasi-continuous lasing. This work will be reported at a later date.

The 2.94 μm operation of the Er:YAG laser is sufficiently interesting to warrant further study. It is a material which can be grown easily and lases well. It has potential application in surgery and as a source to drive a variety of infrared sources at important wavelengths. Since it is compatible with existing Nd:YAG laser systems exploration of its potential is straightforward. As has been pointed out in the present work and in the work of the Soviet scientists, optimum efficiency requires longer duration pump sources and so conversion of Nd:Glass or ruby lasers may lead to better performance. Reliable optical coatings for 2.94 μm requires that they be specified to contain and adsorb no water. As a result of this work it is clear that the Er:YAG laser is available to anyone who wishes to use it.

Acknowledgment

Figure Captions

Fig. 1   A.   Long pulse laser output energy of 33% doped Er:YAG at 2.94 µm versus input energy. Pump pulse duration =120 µsec for o and 170 µsec for ♦.

            B.   Long pulse laser output energy versus input energy for two different Er dopant densities in YAG. o = 33% and ♦ = 50%.

Fig. 2   Energy and power output of the 33% Er:YAG versus pump repetition rate using the 120 µsec duration pump pulse.

Fig. 3   Er:YAG laser waveform near threshold.

Fig. 4   Er:YAG laser waveform at 5 times threshold.

References

[1]E. V. Zharikov, V. I. Zhekov, L. A. Kulevskii, T. M. Murina, V. V. Osiko, A. M. Prokhorov, A. D. Savel'ev, V. V. Smirnov, B. P. Starikov, and M. I. Timoshenko, Sov. J. of Quantum Electronics 4, 1039 (1975)

[2] V. I. Zhekov, V. A. Lobachev, T. M. Murina and A. M. Prokhorov, Sov. J. Quantum Electron. 13, 1235 (1984)

[3]I. A. Scherbakov, General Physics Institute, Moscow, USSR, seminar presented at U.S.C., June 1986

[4] Kh. S. Bagdasarov, V. I. Zhekov, V. A. Lobachev, A. A. Manenkov, T. M. Murina and A. M. Prokhorov, Izvestiya Akademii Nauk SSSR, 48, 1765, (1984)

FIGURE 1

FIGURE 2

SHORT DURATION
PUMP WAVEFORM

LASER WAVEFORM
NEAR THRESHOLD

50 μsec/DIV

10mV

FIGURE 3

LONG DURATION
PUMP WAVEFORM

LASER
DETECTOR
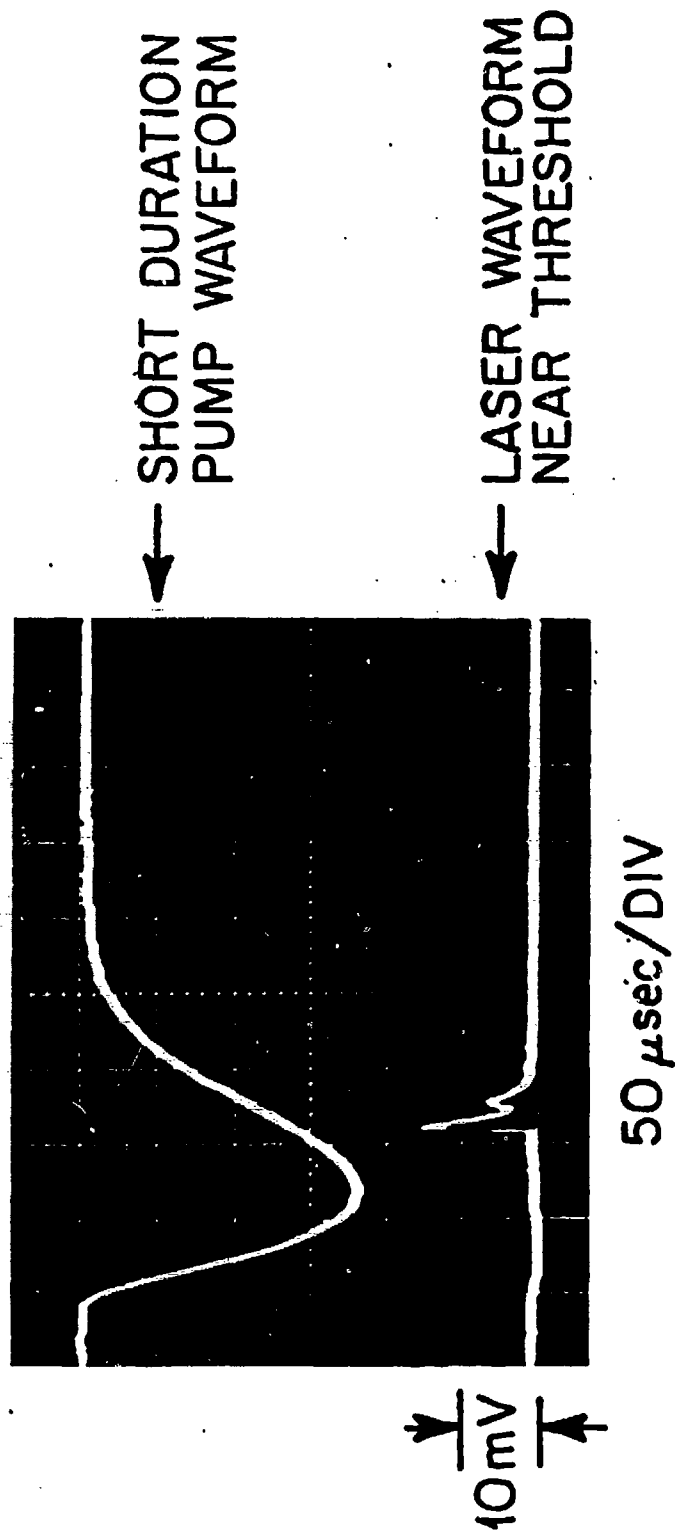SATURATION
VOLTAGE
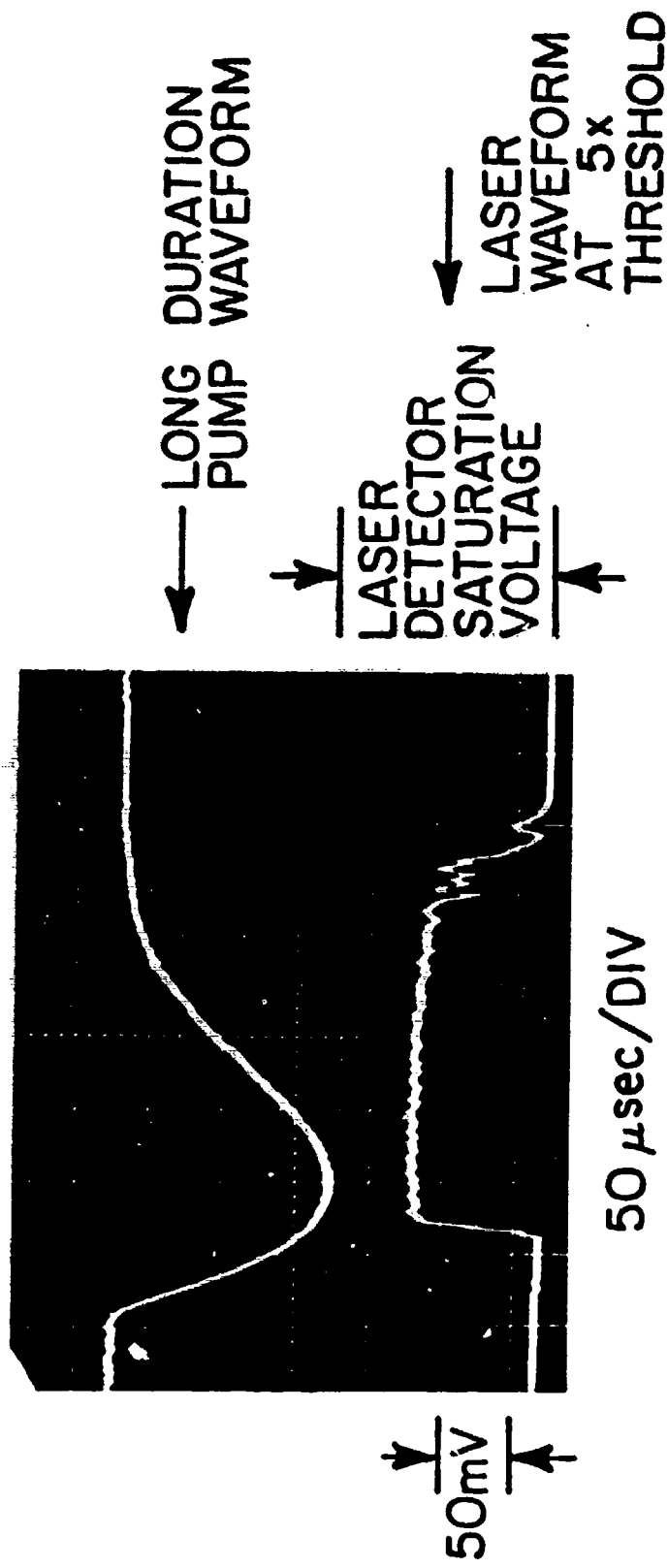
LASER
WAVEFORM
AT 5x
THRESHOLD

50 μsec/DIV

50mV
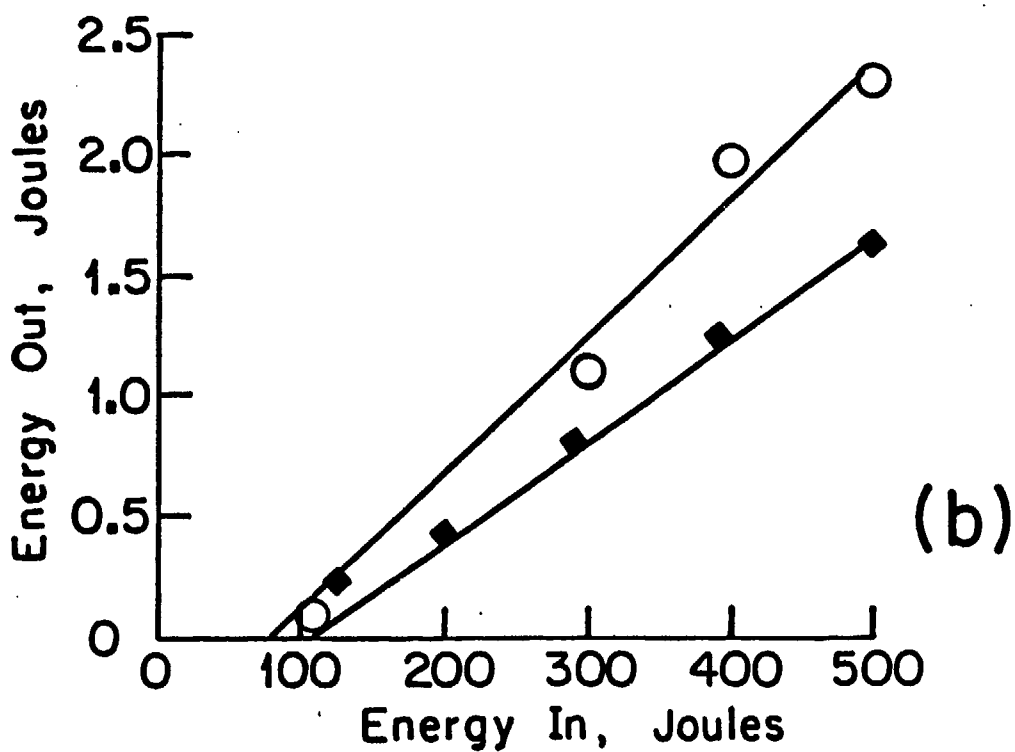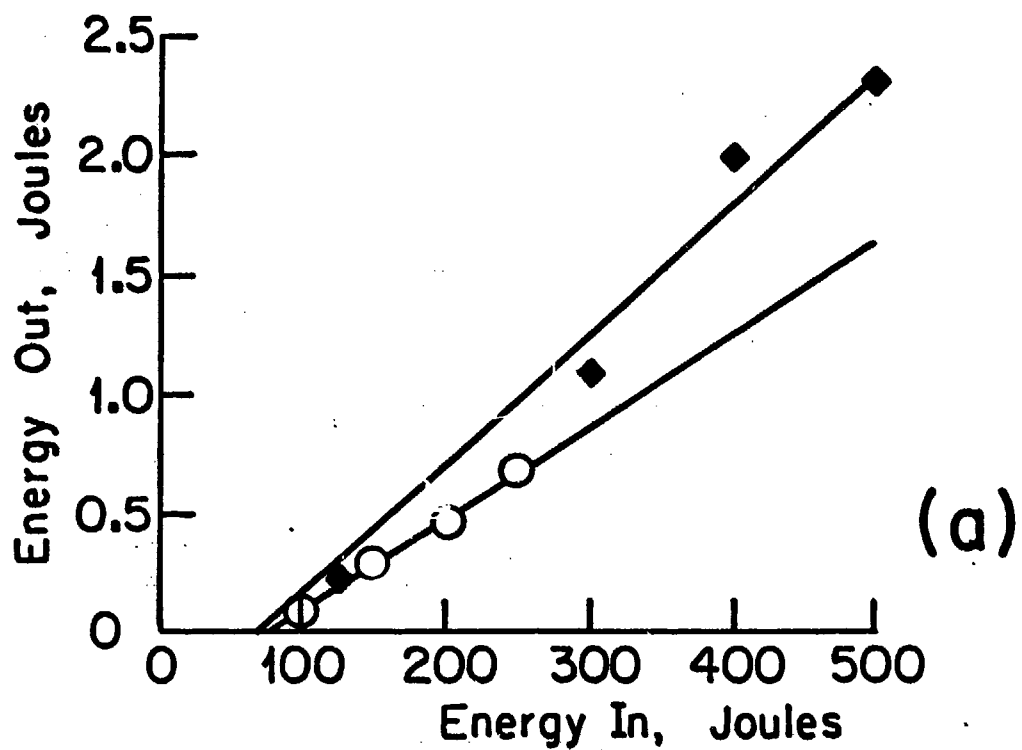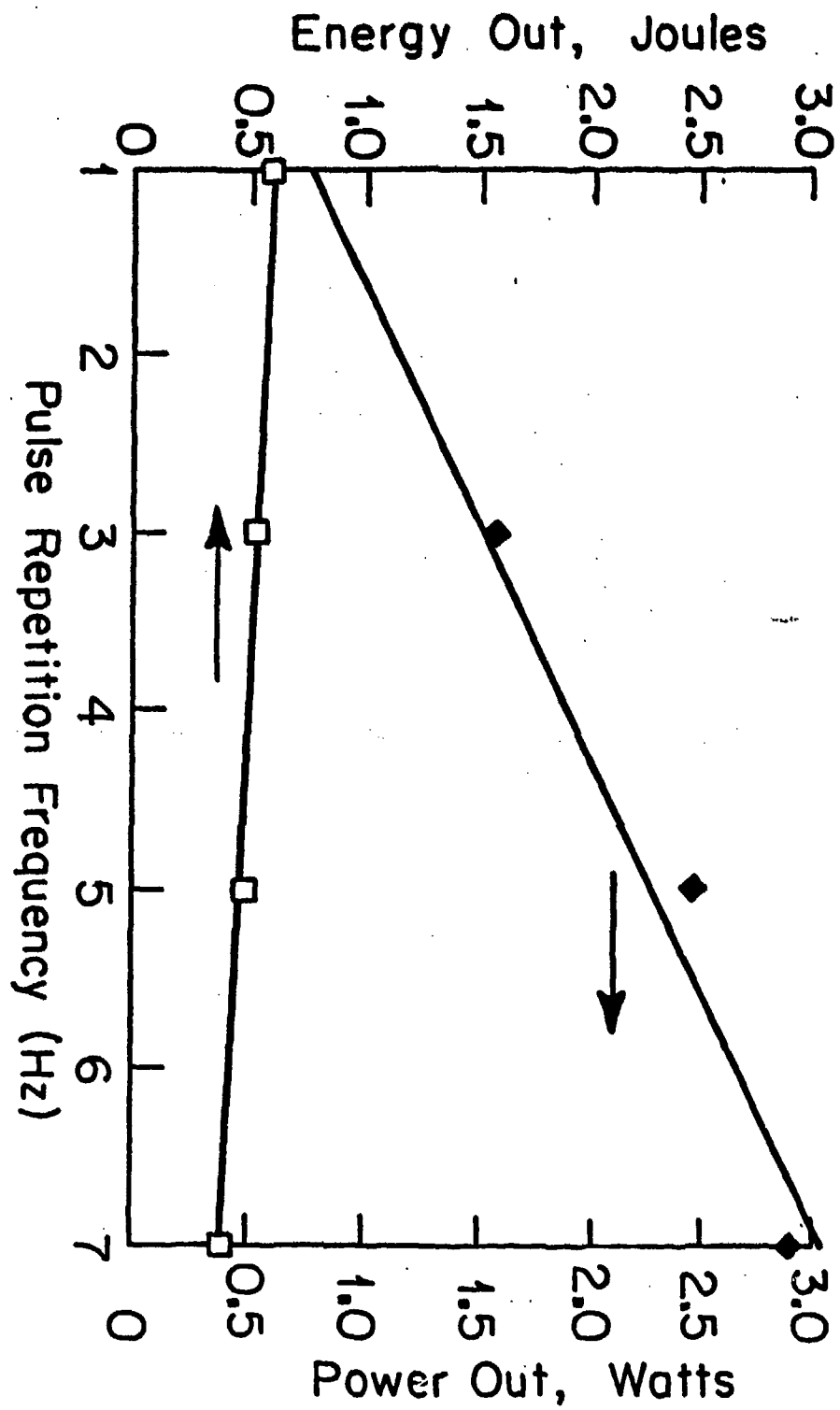
FIGURE 4

HIGHLY EFFICIENT DIODE PUMPED Nd:CRYSTAL LASERS

R. A. Fields, M. Birnbaum, and C. L. Fincher

Electronics Research Laboratory

The Aerospace Corporation

P. O. Box 92957

Los Angeles, CA 90009

(213) 336-6973

Laser diode end-pumped cw operation of Nd:BeL, Nd:YAG, and Nd:YVO$_4$ was compared and evaluated. The lowest threshold, highest slope efficiency (> 53%), and 120 .utput for 1 W electrical input was obtained with Nd:YVO$_4$

SUMMARY

Diode-pumped solid state lasers have become a rapidly growing field as evidenced by their increased presence in the literature as well as their movement into the industrial marketplace. The low thermal stress of diode pumping opens a window of application for many laser materials that have been excluded from more general use due to their poor thermal properties.[1] In this paper we present performance data in a Sipes-type resonator[2] for Nd:BeL and Nd:YVO$_4$, in conjunction with measurements of the accepted standard Nd:YAG.

The spectral differences of the materials studied here have considerable impact on their measurably different thresholds and slope efficiencies. Crystals of similar specifications (dimensions, coatings, doping) were fabricated and measured in the resonator. The comparative power curves of Figure 1 were compiled based on the optimized value of output coupler and diode pump wavelength for each crystal. Nd:YVO$_4$ clearly exhibited the lowest threshold despite its larger optical losses and short fluorescence lifetime (95 µs). To our knowledge, the diode-pumped Nd:YVO$_4$ is the most efficient solid state laser yet demonstrated. The σ_e (emission cross section) of Nd:HVO$_4$ is 2.7 times that of Nd:YAG and greater than 10 times that of Nd:BeL.[3] In the cw pumping configuration, for equal material loss coefficients, the thresholds would be proportional to the $\sigma_e \tau$ products (τ is the fluorescence lifetime). The lower threshold results from the broader absorption band and the higher inversion obtainable in Nd:YVO$_4$. The higher inversion in the vanadate can be traced to the vanadate's emission from the lower sublevel of the $^4F_{3/2}$ where YAG emits from the upper sublevel. We observe better than a 53% slope efficiency for Nd:YVO$_4$ for the high reflector incident optical pump power vs. resonator output. Improvements in the coating (higher pump transmission), beam focus (tighter), and reduction in crystal losses (presently between

1

$0.05 - 0.1$ cm^{-1}) should allow one to approach the complete conversion represented by a 76% slope efficiency for the Nd:YVO$_4$ crystal. Additional experimental details and data will be presented.

The pump wavelength susceptibility of these lasers affects both their efficiency and practicality. A broad continuous absorption band allows for effective pumping from the total emission of the laser diode array. A broad absorption band also permits a greater bandwidth in diode pump wavelengths; thus, for a specified output, a greater number of fabricated diodes will satisfy the necessary pump requirements. The results shown in Figure 2 indicated that Nd:YAG is considerably more sensitive to wavelength changes of the diode output than YVO$_4$ and BeL. The broad continuous bands of Nd:BeL and Nd:YVO$_4$ result in their more efficient pump response.

The σ_e of the 1342 nm band of Nd:YVO$_4$ is slightly greater than that of Nd:YAG at 1064 nm. We will discuss the impact of this for obtaining an efficient diode pumped 1.3 micron laser. Diode pumped Nd:crystal lasers will be analyzed with respect to optimization of their cw and Q-switched operation.
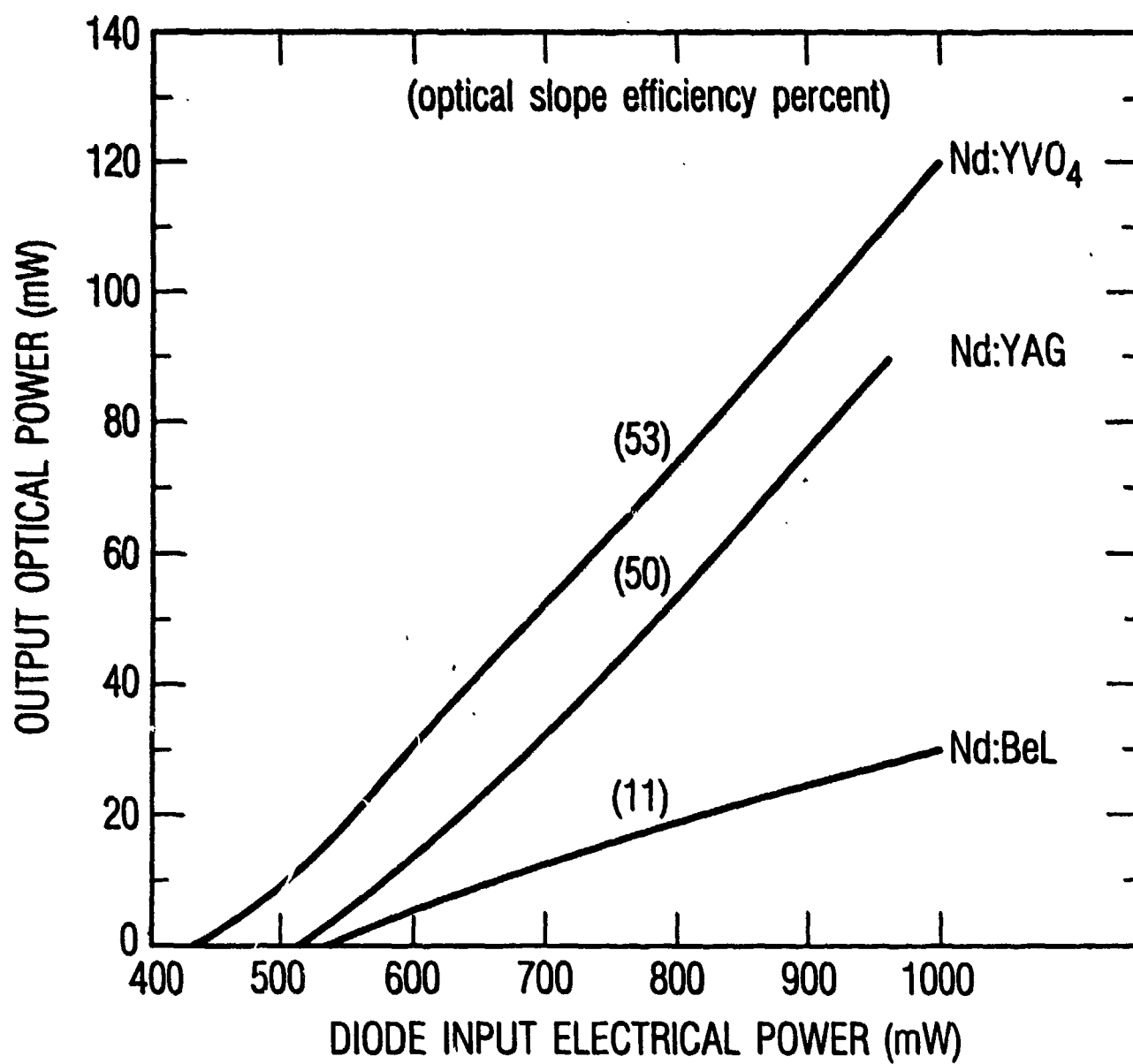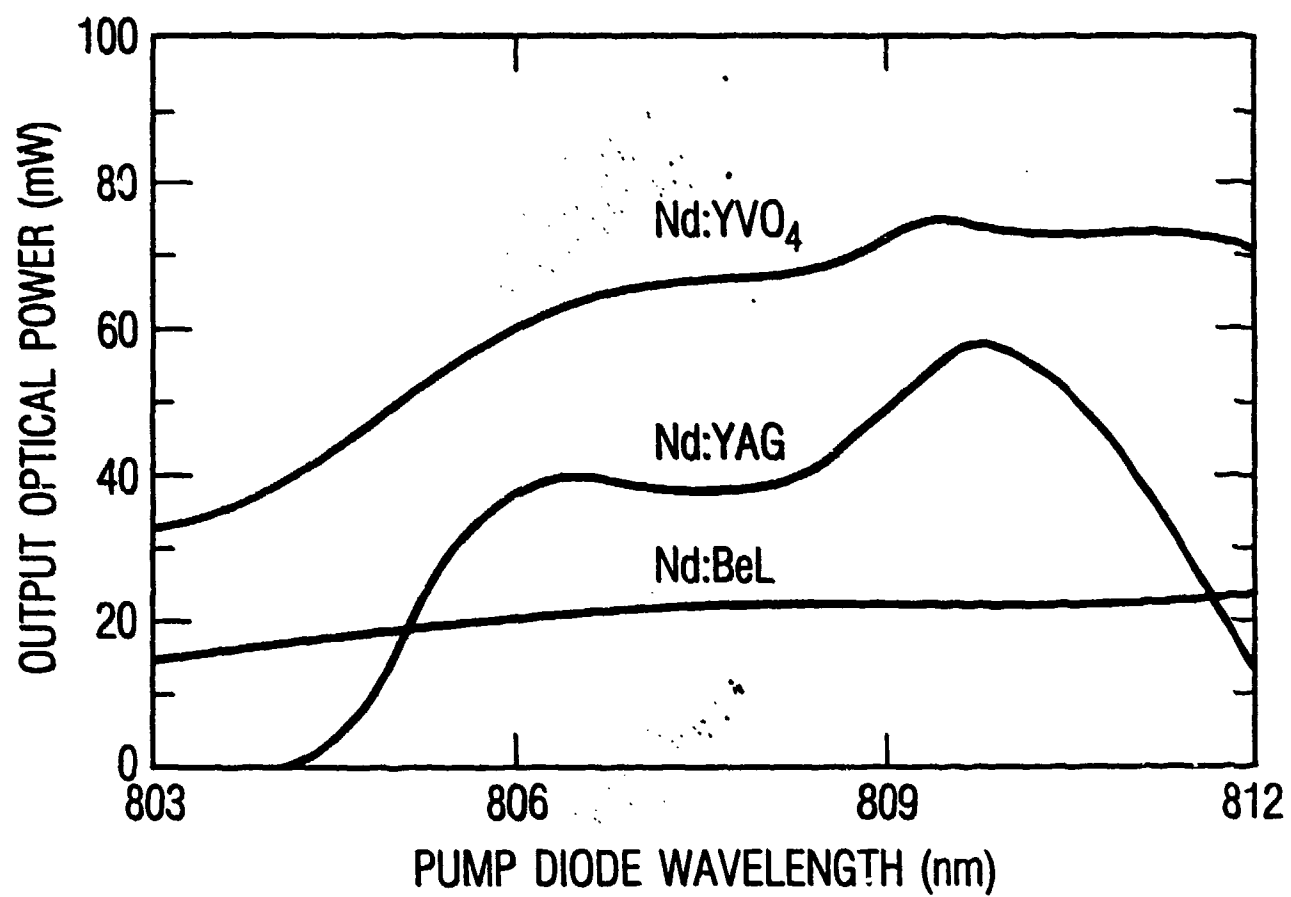
2

REFERENCES

1. W. J. Kozlovsky, T. Y. Fan and R. L. Byer in Technical Digest, Conference on Lasers and Electro-Optics (Optical Society of America, Washington, D. C. (1986), paper WG4.

2. D. Sipes, Appl. Phys. Lett. $\underline{47}$, 75 (1985).

3. A. W Tucker, M. Birnbaum and C. L. Fincher, J. Appl. Phys. $\underline{52}$, 3067 (1981).

4. A. W. Tucker, M. Birnbaum and C. L. Fincher and J. W. Erler, J. Appl. Phys. $\underline{48}$, 4907 (1977).

FIGURE CAPTIONS

Figure 1.   Measured solid state laser output as a function of pump laser
diode electrical input. Optical slope efficiency percents are
in parentheses (YAG and YVO$_4$ at 97%, and BeL at 99% output
couplers).

Figure 2.   Measured solid state laser output as a function of the center
wavelength (approximate) of the diode pump laser array. Optical
pump power was held constant at 167 mW.

4

Figure showing OUTPUT OPTICAL POWER (mW) vs PUMP DIODE WAVELENGTH (nm) for Nd:YVO₄, Nd:YAG, and Nd:BeL.

Laser Material Characteristics of Ti:Al$_2$O$_3$

Milton Birnbaum

Center for Laser Studies

University of Southern California

Los Angeles, CA 90089

(213) 743-7994

Alexander J. Pertica

Now at:

Lawrence Livermore National Lab.

University of California

Livermore, CA 94550

Abstract

Quasi-cw operation of A$^+$-laser pumped Ti:Al$_2$O$_3$ laser crystals has resulted in precision determination of gain and loss coefficients at 780 nm and the first demonstration of the inhomogeneity of the intrinsic material losses.

Laser Material Characteristics of Ti:Al$_2$O$_3$

Milton Birnbaum

Center for Laser Studies

University of Southern California

Los Angeles, CA 90089

(213) 743-7994

Alexander J. Pertica

Now at:

Lawrence Livermore National Lab.

University of California

Livermore, CA 94550

Summary

Quasi-cw laser characteristics of Ti:Al$_2$O$_3$ were obtained utilizing a chopped cw A$^+$ laser pump beam as shown in Fig. 1. This arrangement facilitated the precise alignment of the Ti:Al$_2$O$_3$ rod and resonator for minimum threshold. The low duty cycle employed circumvented the deleterious thermal effects usually encountered in cw pumping.[1] At threshold with plane parallel broad band mirrors peaking at 790 nm, the laser output occurred in a narrow band, less than 10 nm, centered at 780 nm. A typical laser output wavelength band as a function of the pump power is shown in Fig. 2.

The results obtained for three Ti:Al$_2$O$_3$ laser rods are shown in Fig. 3. Utilizing the technique of Birnbaum et al.[2], the data of Fig. 3 was analyzed yielding the stimulated emission cross-section of $2.6 \pm 0.8 \times 10^{-19}$ cm^2 averaged for the three rods. A scanning knife edge method was used to obtain the focussed beam diameter[2]. The intrinsic material losses at 780 nm of rods 1, 3 and 4 were respectively 0.03 cm^{-1}, 0.04 cm^{-1} and 0.035 cm^{-1}. These losses are somewhat greater than has been reported but there is much variability in the quality of the Ti:Al$_2$O$_3$ material.[3]

A unique feature of this study was the determination of the crystal material losses as a function of the position of the pumped filament in the rod. The ratio of high to low intrinsic losses was about 1.5. Our results on the characterization of Ti:Al$_2$O$_3$ laser crystals should prove useful in understanding the origin of the intrinsic material losses and to aid in the attempts to produce homogeneous and low loss Ti:Al$_2$O$_3$.

1

References

1. A. Sanchez, R. E. Fahey, A. J. Strauss and R. L. Aggarwal, "Room Temperature CW Operation of a Ti:Al$_2$O$_3$ Laser," Opt. Lett., Vol. 11, No. 6, 1986, p. 363-5.

2. M. Birnbaum, A. W. Tucker and C. L. Fincher, "Laser Emission Cross Section of Nd:YAG at 1064 nm," J. Appl. Phys., Vol. 52, No. 3, 1981, p. 1212-5.

3. P. Lacovara, L. Esterowitz and M. Kokta, "Growth, Spectroscopy and Lasing of Titanium-Doped Sapphire," IEEE J. of Quant. Electr., Vol. QE 21, No. 10, 1985, p. 1614-8.
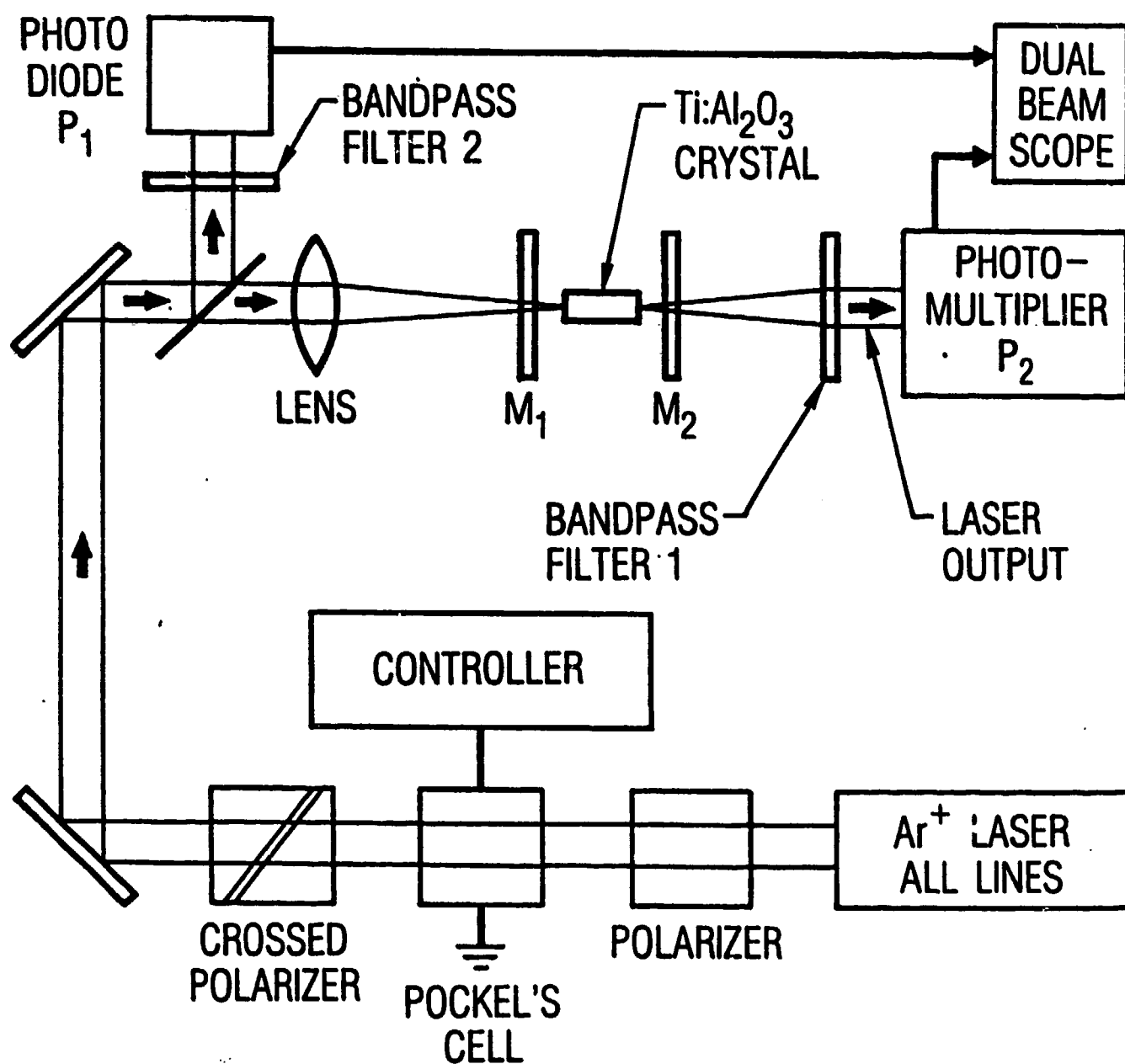
1. Block diagram of experimental arrangement.
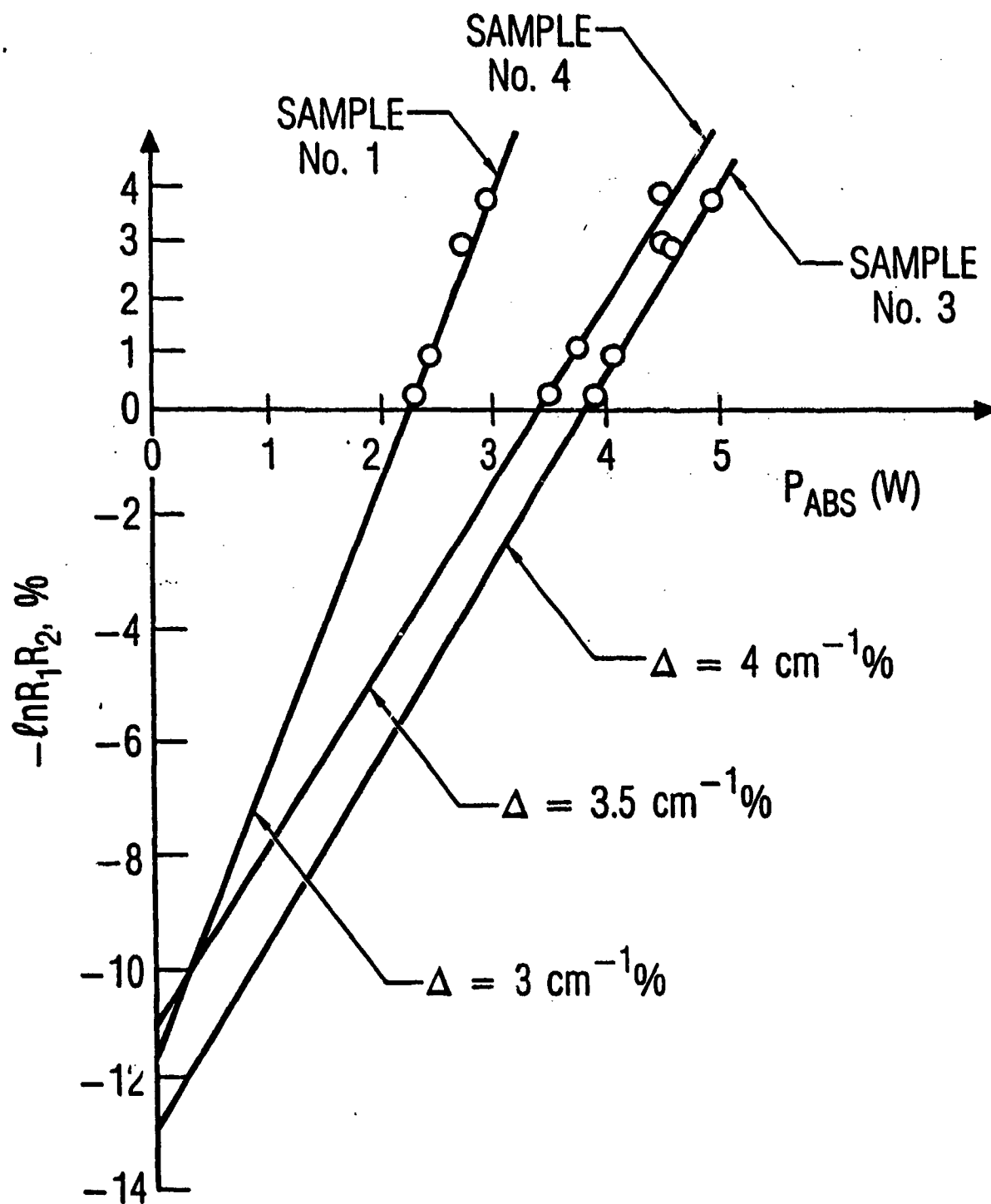
3. Output mirror reflectivity vs. power absorbed at threshold for Ti:Al₂O₃ rods Nos. 1, 3 and 4.

TITANIUM SAPPHIRE
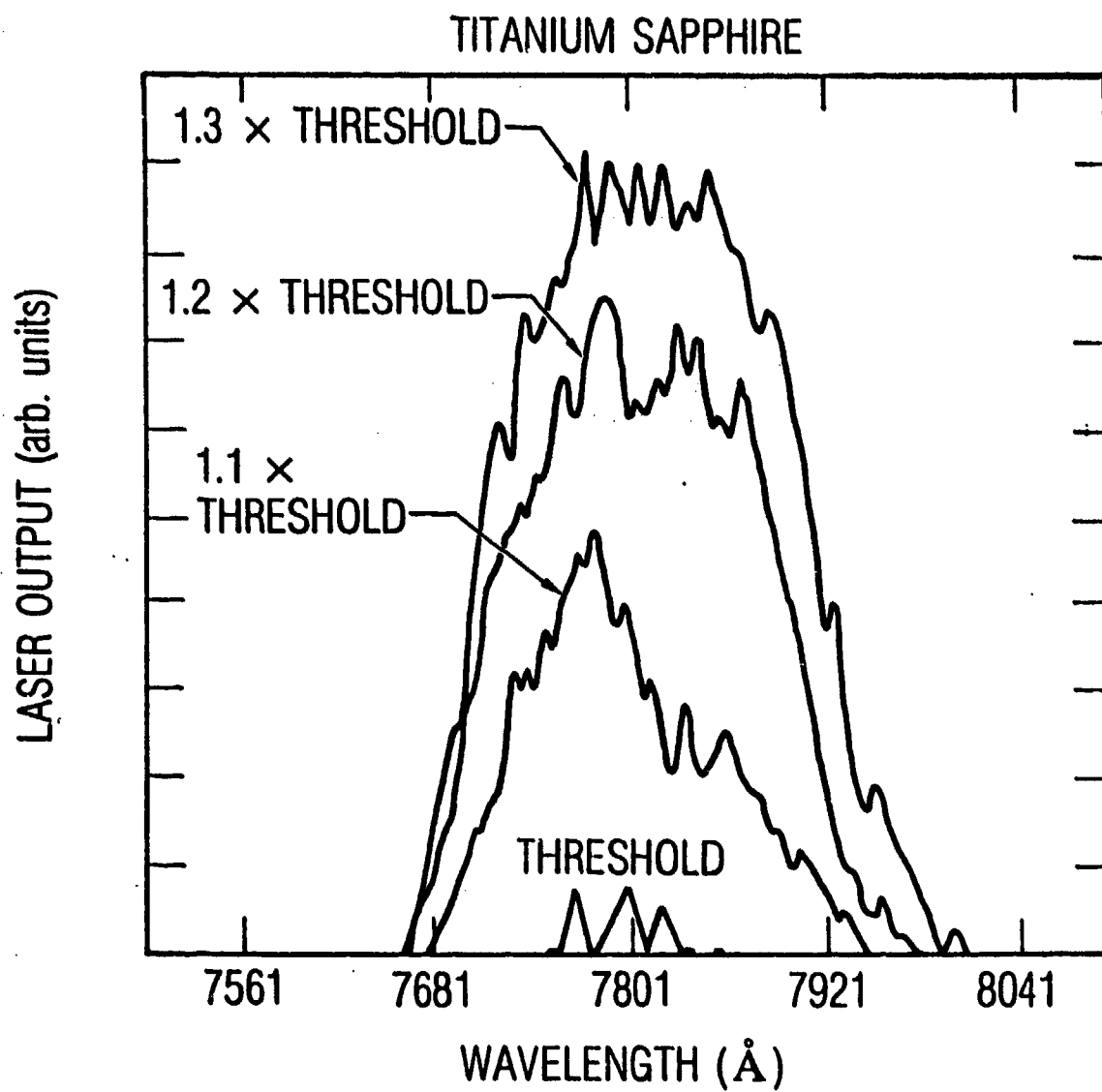
2. Laser output spectrum of rod No. 1, (R₁ = 99.9%, R₂ = 98.0%) as a function of pump power.

Birnbaum and Pertica — "Laser ... Characteristics of Ti:Al$_2$O$_3$"

List of Figure Captions